

# The lid of Pandora's box: geometry near the apparent horizon

Daniel R. Terno

*Department of Physics & Astronomy, Macquarie University, Sydney NSW 2109, Australia and  
Shenzhen Institute for Quantum Science and Engineering, Department of Physics,  
Southern University of Science and Technology, Shenzhen 518055, Guangdong, China*

Trapped regions bounded by horizons are the defining features of black holes. However, formation of a singularity-free apparent horizon in finite time of a distant observer is consistent only with special states of geometry and matter in its vicinity. In spherical symmetry such horizons exist only in two classes of solutions of the Einstein equations. Both violate the null energy condition (NEC) and allow for expanding and contracting trapped regions. However, an expanding trapped region leads to a firewall. The weighted time average of the energy density for an observer crossing this firewall is negative and exceeds the maximal NEC violation that quantum fields can produce. As a result, either black holes only can evaporate or the semiclassical physics breaks down already at the horizons. Geometry of a contracting trapped region approaches the ingoing Vaidya metric with decreasing mass. Only one class of solutions allows for a test particle to cross the apparent horizon, and for a thin shell to collapse into a black hole. These results significantly constrain the regular black hole models. Models with regular matter properties at the horizon can be realized only if significant departures from the semiclassical physics occur already at the horizon scale. The Hayward-Frolov model may describe only evaporation, but not formation of a regular black hole.

## I. INTRODUCTION

Black holes are probably the most celebrated prediction of classical general relativity (GR) [1, 2]. Absence of a fully-developed theory of quantum gravity leaves us with a hierarchy of approximate models that combine GR and quantum mechanics [3]. Quantum effects are known to modify the Einstein equations [3–6] and to enable violations of the classical energy conditions [1–3, 7, 8]. These results make plausible three distinct types of ultra-compact objects (UCOs) models that purport to describe the observed astrophysical black holes [9, 10].

Models of the first type have event horizon and singularity, even if their formation and properties are modified by quantum effects. The final result of their evolution may be a black hole remnant [11]. Another scenario envisages formation of horizonless UCOs. The third option is a black hole that has an apparent horizon, but no event horizon or singularity.

Current observations [12–14] only weakly constrain these scenarios. Given the apparent tension between quantum mechanics and GR, issues of logical consistency of models, as well as the information loss problem [15, 16], it is important to understand what each scenario entails.

There are different opinions on what makes a UCO a black hole [17]. However, the strongest degree of consensus is that it should have a trapped spacetime region, whose boundary is the apparent horizon [1, 2, 12]. A trapped region is a domain where both ingoing and outgoing future-directed null geodesics emanating from a spacelike two-dimensional surface with spherical topology have negative expansion [1, 2, 18]. The apparent horizon is the outer boundary of the trapped region and the defining feature of a physical black hole (PBH) [19, 20]. To be physically relevant the apparent horizon should form in a finite time of a distant observer.

Here we investigate the consequences of having a PBH. The simplest setting to investigate is a spherically-symmetric collapse, where the apparent horizon is unambiguously defined

in all foliations that respect this symmetry [21].

Building on the results of Refs. [20, 22, 23] we describe the two possible classes of the near-horizon geometries, discuss their properties, and consider the implications for singularity-free black hole models.

## II. GEOMETRY NEAR THE APPARENT HORIZON: TWO CLASSES OF SOLUTIONS

We assume validity of semiclassical gravity. That means we use classical notions (horizons, trajectories, etc.), and describe dynamics via the Einstein equations  $G_{\mu\nu} = 8\pi T_{\mu\nu}$ , where the standard left-hand side is equated to the expectation value  $T_{\mu\nu} = \langle \hat{T}_{\mu\nu} \rangle_\omega$  of the renormalized energy-momentum tensor (EMT). The latter represents both the collapsing matter and the created excitations of the quantum fields. We do not assume existence of the Hawking radiation or specific properties of the state  $\omega$ .

Boundaries of the trapped region are nonsingular in classical GR [1, 2], a requirement that is typically assumed to extend to the semiclassical regime. We implement this property by requiring that the scalars  $\mathcal{T} := T^\mu{}_\mu$  and  $\mathcal{I} := T^{\mu\nu}T_{\mu\nu}$  are finite. The Einstein equations imply that  $64\pi^2\mathcal{I} = R_{\mu\nu}R^{\mu\nu}$  and  $8\pi\mathcal{T} = -R$ , where  $R_{\mu\nu}$  and  $R$  are the Ricci tensor and the Ricci scalar, respectively. Finite values of these scalars are a necessary regularity condition, and additional tests may be required.

A general spherically-symmetric metric in the Schwarzschild coordinates is given by

$$ds^2 = -e^{2h(t,r)}f(t,r)dt^2 + f(t,r)^{-1}dr^2 + r^2d\Omega, \quad (1)$$

where  $r$  is the areal radius. The Misner-Sharp mass [12, 18, 24]  $C(t, r)$  is invariantly defined via

$$1 - C/r := \partial_\mu r \partial^\mu r, \quad (2)$$

and thus the function  $f(t, r) = 1 - C(t, r)/r$  is invariant under general coordinate transformations. The apparent horizon

is located at the Schwarzschild radius  $r_g$  that is the largest root of  $f(t, r) = 0$  [18, 21]. The function  $h(t, r)$  may contain information about potential hairs of the stationary PBHs [2, 25], and plays the role of an integrating factor in the coordinate transformations.

It is convenient to introduce

$$\tau_t := e^{-2h} T_{tt}, \quad \tau^r := T^{rr}, \quad \tau_t^r := e^{-h} T_t^r, \quad (3)$$

and represent the Misner-Sharp mass as

$$C = r_g(t) + W(t, r - r_g), \quad (4)$$

where the definition of the apparent horizon implies

$$W(t, 0) = 0, \quad W(t, x) < x. \quad (5)$$

In this notation the three Einstein equations for  $G_{tt}$ ,  $G_r^t$ , and  $G^{rr}$  become

$$\frac{\partial_r C}{r^2} = 8\pi \frac{\tau_t}{f}, \quad (6)$$

$$\frac{\partial_t C}{r^2} = 8\pi e^h \tau_t^r, \quad (7)$$

$$\frac{\partial_r h}{r} = 4\pi \frac{(\tau_t + \tau^r)}{f^2}, \quad (8)$$

respectively.

Regularity of the apparent horizon is expressed as a set of conditions on the potentially divergent parts of the curvature scalars. For  $\mathbb{T}$  and  $\mathbb{T}$  these are

$$\mathbb{T} = (\tau^r - \tau_t)/f \rightarrow g_1(t) f^{\kappa_1}, \quad (9)$$

$$\mathbb{T} = ((\tau^r)^2 + (\tau_t)^2 - 2(\tau_t^r)^2)/f^2 \rightarrow g_2(t) f^{\kappa_2}, \quad (10)$$

for some  $g_{1,2}(t)$  and  $\kappa_{1,2} \geq 0$ . Here we exclude  $T_\theta^\theta \equiv T_\phi^\phi$  from consideration, because the Einstein equations imply that  $T_\theta^\theta$  is finite (Appendix A 1).

Eqs. (9) and (10) require the EMT components to scale as some power  $f^k$  as  $r$  approaches the apparent horizon at  $r_g$ . All spherically-symmetric PBH solutions can be classified by the values of  $k$ . Only the classes  $k = 0$  (that results in the divergent energy density and pressure at the apparent horizon) and  $k = 1$  (finite non-zero values of energy density and pressure at the apparent horizon) are self-consistent. They are described below.

Using the advanced and the retarded null coordinates allows additional insights into the near-horizon geometry. Its description in the terms of the advanced null coordinate  $v$ ,

$$dt = e^{-h}(e^{h+} dv - f^{-1} dr), \quad (11)$$

is useful in the case of contracting apparent horizon,  $r_g' < 0$ . A general spherically-symmetric metric in  $(v, r)$  coordinates is

$$ds^2 = -e^{2h+} \left(1 - \frac{C_+}{r}\right) dv^2 + 2e^{h+} dv dr + r^2 d\Omega. \quad (12)$$

If  $r_g' > 0$  it is useful to employ the retarded null coordinate  $u$ .

Imposing the finiteness conditions on the Ricci scalar  $R$  (Appendix A 2) at the apparent horizon  $r_+(v) \equiv C_+(v, r_+) = r_g(t)$ , we obtain that as  $r \rightarrow r_g \equiv r_+$ ,

$$C_+(v, r) = r_+(v) + w_+(v)(r - r_+) + w_2^+(r - r_+)^2 \dots, \quad (13)$$

$$h_+(v, r) = \chi_+(v)(r - r_+) + \dots, \quad (14)$$

for some functions  $w_+$ ,  $w_2$  and  $\chi_+$ , where the condition  $w_+ \leq 1$  follows from the requirement  $C < r$  outside the Schwarzschild radius.

Components of the EMT are related by

$$\theta_v := e^{-2h+} \Theta_{vv} = \tau_t, \quad (15)$$

$$\theta_{vr} := e^{-h+} \Theta_{vr} = (\tau_t^r - \tau_t)/f, \quad (16)$$

$$\theta_r := \Theta_{rr} = (\tau^r + \tau_t - 2\tau_t^r)/f^2, \quad (17)$$

where  $\Theta_{\mu\nu}$  denote the EMT components in  $(v, r)$  coordinates. The limits  $\theta_{\mu\nu}^+ := \lim_{r \rightarrow r_+} \theta_{\mu\nu}$  are

$$\theta_v^+ = (1 - w_+) \frac{r_+'}{8\pi r_+^2}, \quad \theta_{vr}^+ = -\frac{w_+}{8\pi r_+^2}, \quad \theta_r^+ = \frac{\chi_+}{4\pi r_+}. \quad (18)$$

## A. Divergent density and pressure

Regularity conditions of Eqs. (9) and (10) require that divergent terms in the curvature scalars must cancel. Adding the requirement that the function  $C(t, r)$  is a real solution of Eq. (6) results in

$$\tau_t = \tau^r = -\Upsilon^2(t) f^k, \quad \tau_t^r = \pm \Upsilon^2 f^k, \quad (19)$$

where  $\Upsilon^2(t)$  is some function of time,  $k < 1$ , and the higher-order terms are omitted. In the orthonormal basis the  $(\hat{t}\hat{r})$  block of the EMT is

$$T_{\hat{a}\hat{b}} = -\Upsilon^2 f^{k-1} \begin{pmatrix} 1 & \pm 1 \\ \pm 1 & 1 \end{pmatrix}. \quad (20)$$

The upper (lower) signs of  $T_{\hat{t}\hat{r}}$  correspond to growth (evaporation) of the PBH. Leading terms of the solutions for  $C(t, r)$  and  $h(t, r)$  are given in Appendix A 3. Static non-vacuum solutions with  $\tau_t^r \rightarrow 0$  are impossible for  $k < 1$ , as the regularity condition Eq. (10) cannot be satisfied unless all three components are zero.

The null energy condition (NEC) requires  $T_{\mu\nu} l^\mu l^\nu \geq 0$  for all null vectors  $l^\mu$ . It is violated for all values of  $k < 1$  by radial vectors  $l^{\hat{a}} = (1, \mp 1, 0, 0)$  for the evaporating and the accreting PBH solutions, respectively

Violations of the NEC are bounded by quantum energy inequalities (QEIs) [8, 26]. For a growing PBH,  $r_g' > 0$ , in the reference frame of an infalling massive test particle the energy density (as well as the pressure and the flux), diverge (Appendix B 1). Such a transient firewall leads to a violation of the quantum energy inequality [8, 27], that is shown by repeating the analysis of Ref [23]. Henceforth we consider only the solutions with  $r_g' < 0$ .

Comparison of Eqs. (15) – (18) with Eq. (19) shows that only the case  $k = 0$  is allowed, with  $\Upsilon^2 = -\theta_v^+$ . Solutions with  $k < 0$  are incompatible with Eq. (15). Solutions with  $0 < k < 1$  are excluded by following the chain of reasoning that leads to Eqs. (25)–(27) (Appendix A 3).

For  $k = 0$  the leading terms in the metric functions in  $(t, r)$  coordinates are given as power series in terms of  $x := r - r_g$  as

$$C = r_g - w\sqrt{x} + \frac{1}{3}x \dots, \quad h = -\frac{1}{2} \ln \frac{x}{\xi} + \frac{4}{3w}\sqrt{x} + \dots, \quad (21)$$

where  $w^2 := 16\pi\Upsilon^2 r_g^3$  and the higher-order terms depend on the higher-order terms in the EMT expansion [22]. The function  $\xi(t)$  is determined by the choice of the time variable. The metric functions  $C$  and  $h$  are obtained as the solutions of Eqs. (6) and (8), respectively. Eq. (7) must then hold identically. Both of its sides contain terms that diverge as  $1/\sqrt{x}$ . Their identification results in the consistency condition

$$r'_g/\sqrt{\xi} = \pm 4\sqrt{\pi}\Upsilon\sqrt{r_g} = \pm w/r_g. \quad (22)$$

A static observer finds that the energy density  $\rho = -T_t^t$ , the pressure  $p = T_r^r$ , and the flux diverge at the apparent horizon. On the other hand, in the reference frame of the infalling observer on an arbitrary radial trajectory  $(T_A(\tau), R_A(\tau), 0, 0)$  these quantities are

$$\rho_A = p_A = \phi_A = -\frac{\Upsilon^2}{4\dot{R}^2}, \quad (23)$$

at the horizon crossing. Additional properties of this metric are discussed in Refs. [20, 23]

Further relations between the EMT components near the apparent horizon are obtained as follows. A point on the apparent horizon has the coordinates  $(v, r_+)$  and  $(t, r_g)$  in the two coordinate systems. Moving from  $r_+(v)$  along the line of constant  $v$  by  $\delta r$  leads to the point  $(t + \delta t, r_g + \delta r)$ . Eqs. (11) and (22) imply

$$\delta t = -\left. \frac{e^{-h}}{f} \right|_{r=r_g} \delta r = -\frac{r_g \delta r}{\sqrt{\xi} w} = \frac{\delta r}{r'_g}. \quad (24)$$

Hence the EMT components are related at the first order in  $\delta r$  by

$$\partial_r \theta_v^+ = -2\Upsilon\Upsilon'/r'_g + \alpha, \quad (25)$$

$$\partial_r \theta_v^+ + \frac{1-w_+}{r_+} \theta_{vr}^+ = -2\Upsilon\Upsilon'/r'_g + \beta, \quad (26)$$

$$\partial_r \theta_v^+ + 2\frac{1-w_+}{r_+} \theta_{vr}^+ = -2\Upsilon\Upsilon'/r'_g + \gamma, \quad (27)$$

where  $\partial_r \theta_v^+ := \partial_r \theta_v|_{r_+}$ ,  $\alpha(t) := \partial_r \tau_t|_{r_g}$ ,  $\beta := \partial_r \tau_t^r|_{r_g}$ ,  $\gamma := \partial_r \tau^r|_{r_g}$ . As a result, the subleading terms satisfy

$$\alpha + \gamma = 2\beta. \quad (28)$$

This metric approaches the pure ingoing Vaidya metric with decreasing mass, which is the usual near-horizon approximation when the backreaction from Hawking radiation is taken into account [28, 29]. The triple limit  $\tau_t, \tau^r, \tau_t^r \rightarrow -\Upsilon^2$  is observed in the *ab initio* calculations of the renormalized energy-momentum tensor on the Schwarzschild background [30].

## B. Finite density and pressure

For  $k \geq 1$  Eqs. (9) and (10) do not impose any constraints, and different components of the energy-momentum tensor can converge to zero at different rates. However, only the case  $k = 1$ , where at the leading order in  $f$

$$\tau_t = E(t)f, \quad \tau^r = P(t)f, \quad \tau_t^r = \Phi(t)f, \quad (29)$$

allows for a solution with  $r'_g \neq 0$  (see Appendices A 4 and B 3 for details). These solutions exhibit a finite pressure and a finite density at the apparent horizon,  $\rho(t, r_g) = E$  and  $p(t, r_g) = P$ , respectively.

Then Eq. (6) results in the Misner-Sharp mass

$$C = r_g(t) + 8\pi E r_g^2 x + \dots, \quad 8\pi E r_g^2 < 1. \quad (30)$$

The strict inequality follows from Eq. (34) below, as  $8\pi r_g^2 E = 1$  is incompatible with  $r'_g \neq 1$ . Consistency of Eqs. (7) and (8) results in

$$\frac{4\pi(E+P)r_g^2}{1-8\pi E r_g^2} = -1, \quad (31)$$

that ensures the necessary logarithmic divergence of  $h$ ,

$$h = -\ln \frac{x}{\xi(t)} + \omega(t)x + \dots, \quad (32)$$

for some  $\xi(t) > 0$  and  $\omega(t)$ . As a result, Eq. (7) relates the rate of change of the Schwarzschild radius and the flux as

$$r'_g = 8\pi\Phi\xi r_g. \quad (33)$$

Requiring the Ricci scalar to be finite at  $r_g$  (Appendix B 4) imposes the constraint

$$(1-8\pi E r_g^2)\xi = \pm r'_g r_g, \quad (34)$$

where the upper (lower) signs corresponds to the expansion (contraction) of the apparent horizon.

The above conditions imply that a single quantity determines the two other parameters at the apparent horizon,

$$P = \frac{-1+4\pi E r_g^2}{4\pi r_g^2}, \quad \Phi = \pm \frac{1-8\pi E r_g^2}{8\pi r_g^2}, \quad (35)$$

where the upper (lower) sign corresponds to accretion (evaporation). The  $(t, r)$  block of the EMT is given in Appendix B 2. The NEC is violated in both cases. For example, for  $r'_g < 0$  and the outward pointing null vector  $k^\mu$  as  $r \rightarrow r_g$

$$T_{\mu\nu} k^\mu k^\nu \approx -\frac{1}{2\pi r_g x}. \quad (36)$$

For  $\Phi > 0$  (an accreting trapped region,  $r'_g > 0$ ) in the reference frame of an infalling observer the energy density diverges. This transient firewall leads to the violation of the QEI, similarly to the  $k = 0$  case (Appendix B 2).

The metric of Eq. (12) describes the  $k = 1$  evaporating black hole only if  $w_+ \equiv 1$ . Compatibility with Eqs. (16) and (17) results in the relations

$$8\pi r_g^2(E - \Phi) = 1, \quad E + P - 2\Phi = 0, \quad (37)$$

that are automatically satisfied due to Eq. (35).

Consider now a time-independent apparent horizon, so the PBH is neither accreting nor evaporating, while the solution is still time-dependent (such solutions were considered in the framework of modified gravity, e.g., in [34]). We treat it as a limiting case of evaporation,  $\Phi \leq 0$ . The condition  $r'_g = 0$  requires

$$\frac{4\pi(E + P)r_g^2}{1 - 8\pi E r_g^2} = -\lambda, \quad (38)$$

$\lambda < 1$  to hold. The Ricci scalar is finite only if either the density takes the extreme allowed value  $E = (8\pi r_g^2)^{-1}$ , or  $\lambda = \frac{1}{2}$  (Appendix B 4). Using Eq. (37) (that still holds up to the end of the dynamical phase), we obtain

$$\Phi = 0, \quad E = -P = 1/(8\pi r_g^2), \quad (39)$$

in both cases. The NEC is not violated so the solution cannot be realized in finite time  $t$ .

A static solution with all metric function being independent of time is possible only if  $\tau'_t \equiv 0$ . If  $h \neq 0$  there is no general requirement  $\rho = -p$ , but Eqs. (25)–(27) imply  $E = -P$ .

### C. Crossing the apparent horizon

Both massless sufficiently fast ( $4\pi r_g^2 \Upsilon^2 < \dot{R}^2$ ) massive test particles cross the apparent horizon of  $k = 1$  PBH in finite time of a distant observer [23]. However, it is impossible to fall into a  $k = 1$  black hole.

Consider for simplicity a massless test particle. It is convenient to parameterize the radial ingoing null geodesic  $(T_A, R_A)$  by its radial coordinate,  $\lambda = -R_A$ . Possibility of the horizon crossing is conveniently monitored by the gap function [31, 32],

$$X(\lambda) := R_A - r_g(T_A(\lambda)), \quad (40)$$

whose negative rate of change  $X_\lambda = dX/d\lambda = -1 - r'_g dT_A/d\lambda$  indicates that the particle keeps approaching the apparent horizon.

Noting that

$$\frac{dT_A}{d\lambda} = \frac{e^{-h(T_A, R_A)}}{f(T_A, R_A)} = \frac{r_g}{\xi} \frac{1 - (\omega - r_g^{-1})X}{1 - 8\pi E r_g^2} + \mathcal{O}(X^2). \quad (41)$$

Similarly, the rate of change of the coordinate time with respect to the proper time of an infalling massive test particle is also finite. Expanding  $X(\lambda)$  in powers of  $X$  we find that

$$X_\lambda = -(\omega - r_g^{-1})X + \mathcal{O}(X^2). \quad (42)$$

If  $(\omega - r_g^{-1}) < 0$ , then once certain minimal coordinate distance is reached the gap has to increase. If  $(\omega - r_g^{-1}) > 0$ , then the gap will close exponentially slow,

$$X \approx X_0 \exp\left(-\int_{\lambda_0}^{\lambda} (\omega - r_g^{-1}) d\lambda\right), \quad (43)$$

and thus crossing of the apparent horizon ( $X = 0$ ) of an evaporating  $k = 1$  PBH never happens. The same conclusion is obtained by considering a massive test particle and the proper time parametrization.

These results cast doubts on the possibility that  $k = 1$  black holes can actually form. A thin dust shell, with a flat metric inside and a curved metric outside, provides the simplest tractable model of the collapse. The classical Schwarzschild exterior leads to the well-known result of a finite proper time of the collapse and an infinite collapse time  $t$  according to the clock of a distant observer. By using the Vaidya metrics to emulate the effects of evaporation, one obtains results that depend on their choice [22].

By assuming the outgoing Vaidya metric with decreasing mass (which satisfies the NEC and thus cannot lead to the formation of a PBH in finite coordinate time  $t$ ), the apparent horizon is never formed, but the shell either becomes superluminal [33] or develops a surface pressure at the coordinate distance  $x \sim w^2$  from the Schwarzschild radius [22, 32]. On the other hand, the ingoing Vaidya metric of Eq. (12) leads to the horizon formation in finite time according to both clocks [22]. However, if the exterior is modelled by Eq. (1) with  $k = 1$  metric functions (Eqs. (30) and (32)), Eq. (43) indicates that the shell's collapse will never be complete, even if the exterior metric violates the NEC.

## III. IMPLICATIONS FOR MODELS OF REGULAR BLACK HOLES

Whether their motivation is to construct a geodetically complete spacetime, to resolve the information loss paradox, or to illustrate the effects of quantum gravity, models of regular black holes (RBHs) envisage a trapped region with a singularity-free core (see e.g., [35–40] and the reviews [11, 41, 42]). Considerations of a geometric nature [43], as well as constraints from the effective field theory of quantum gravity [44, 45] restrict these models. Here we explore the further constraints that are imposed by the results of Sec. II.

Many of the proposed static models [35, 37, 39] assume finite density and pressure at the horizon and thus belong to the class  $k = 1$ . However, such solutions cannot be realized without a breakdown of the semiclassical physics. Leaving aside the doubts about viability of the dynamical  $k = 1$  solutions, the static situation ( $E = -P$ ,  $\Phi = 0$ ) still cannot arise at finite  $t$ , as in this case the NEC is satisfied and the apparent horizon is hidden from the distant observer by the event horizon. Appearance of the feature that the model is built to prevent indicates its breakdown.

Even the asymptotic case cannot be realized without some radical departures from the semiclassical physics. The zero

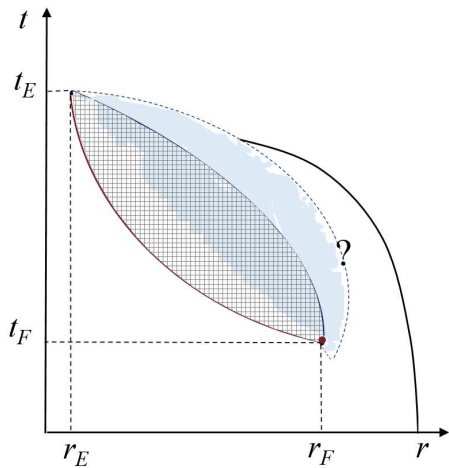


FIG. 1. Schematic depiction of the evolution of a RBH from the point of view of a distant observer. The dark blue line represents the apparent horizon and the double dark red line represents the inner horizon. The trapped region is cross-hatched. The NEC-violating region (blue spread, dashed boundary) appears prior to the formation of the first marginally trapped surface  $(t_F, r_F)$  and covers part of the trapped region. Its outer boundary is not constrained by our considerations. The thin black line traces the surface of the collapsing body up to the NEC-violating region. The trapped region evaporates at some  $(t_E, r_E)$  where the two hypersurfaces cross again.

flux limit can be produced only if the scenario of Eq. (39) is realized. However, in the limit  $8\pi r_g^2 E \rightarrow 1$  the formerly regular terms in the curvature scalars diverge (Appendix B 4).

The leading behaviour of the function  $h$  of the  $k = 0$  solutions matches the regular static scenario with  $k = 1$ ,  $\lambda = \frac{1}{2}$ . Nevertheless, the latter is not a suitably defined limit of the former. First, to produce this effect some mechanism should freeze the apparent horizon and thus push  $\Upsilon$  in  $\tau_t = -\Upsilon^2 + \alpha x + \dots$ , etc., to zero. This is exactly opposite of the expected semiclassical behavior [2, 16, 29]. Moreover, after the freezing, to avoid a discontinuous change in the black hole (Misner-Sharp) mass, the linear terms in Eqs. (21) and (30) should match. This leads to a contradiction

$$E = \frac{1}{24\pi r_g^2} \neq \frac{1}{8\pi r_g^2} = -P, \quad (44)$$

where the first value of  $E$  is obtained by matching with the linear part of Eq. (21) and the second value results from Eq. (39).

A dynamical model of Hayward and Frolov [37, 38] uses  $(v, r)$  coordinates and the minimal modification of the Vaidya metric by setting

$$C_+(v) = \frac{2m(v)r^3}{r^3 + 2m(v)b^2}, \quad h_+ = 0, \quad (45)$$

for some  $b > 0$  and  $m(v)$ . When  $m \gg b$  the approximate locations of the apparent horizon and the inner horizon are given by

$$r_g \approx 2m - \frac{b^2}{2m}, \quad r_{in} \approx \frac{5b}{4} - \frac{3b^2}{32m}, \quad (46)$$

respectively, and the non-zero components of the energy-momentum tensor at the apparent horizon are

$$\Theta_{vv} \approx \frac{m'(v)}{16\pi m^2(v)}, \quad \Theta_{vr} \approx -\frac{3b^2}{128m^4}. \quad (47)$$

This model belongs to  $k = 0$  class. It is consistent with formation of the apparent horizon at a finite time of a distant observer.

However, it is a consistent description of only the evaporation part of the RBH evolution and cannot describe its formation. Leaving aside the issue of a transient firewall that accompanies accretion, for  $m'(v) > 0$  the NEC is not violated in this model. Thus the apparent horizon, if exists, is hidden behind the even horizon that was purportedly eliminated. In fact, no model that uses  $(v, r)$  coordinates and has a regular function  $h_+(v, r)$  can describe growth of a PBS, as in this case  $\tau_t^r \rightarrow +\Upsilon^2$

$$\frac{\partial_r h_+}{r} = 4\pi \Theta_{rr}^+ \rightarrow \frac{16\pi}{f^2} \Upsilon^2, \quad (48)$$

that ensures divergence of at least of  $\partial_r h_+$ .

Since the energy density and pressure are negative in the vicinity of the apparent horizon and positive in the vicinity of the inner horizon [19, 23] there should be density and pressure jumps at the intersection of the two horizons, making problematic the blanket requirement of continuity of density and pressure. If we accept that violations of the QEI is a sufficient reason to discount the growth of trapped region, the horizon structure of a regular black hole is schematically shown on Fig. 1.

In this case the model with the metric functions (45) cannot describe the first stages of the evolution of the trapped region, even if  $C'_+ < 0$ . For a RBH of Fig. 1 both the apparent horizon and the inner horizon develop from a single trapped surface that appears at some  $t_F$  and meet again at  $t_E$ , possibly forming a remnant. The Misner-Sharp mass of Eq. (45) allows a latter possibility (at  $m(v_E) = 3\sqrt{3}b/4$ ), but not the former one, as Eq. (46) indicates.

#### IV. DISCUSSION

We have seen that in the vicinity of the apparent horizon a singular nature of Schwarzschild coordinates serves a useful purpose. Scaling of the suitably selected functions of the EMT components with the powers  $k$  of  $f = (1 - C(t, r)/r)$  allows to classify solutions of the Einstein equations. Only two types of solutions with  $k = 0, 1$  are possible. Both violate the NEC and result in a firewall at the expanding apparent horizon. Only  $k = 0$  solutions allow to a collapsing thin shell to form a black hole or for a test particle to cross the apparent horizon. These failures cast doubts on the physical relevance of the  $k = 1$  solutions.

Analysis of the inner regions of RBHs leads to the arguments indicating the need for physics beyond standard model to support such objects [40, 46]. Our analysis of the near-horizon regions indicates that  $k = 0$  models of evaporating

RBHs are as exotic as any UCO with or without an apparent horizon. On the other hand, complete regularity (finite values of density and pressure for both static and infalling observers) of  $k = 1$  PBH may be impossible to realize without significant modification of the semiclassical gravity.

## ACKNOWLEDGMENTS

Useful discussions with Valentina Baccetti, Robert Mann and Sebastian Murk are gratefully acknowledged.

### Appendix A: Solutions with $k < 1$

#### 1. Behaviour of $T_\theta^\theta$

The regularity conditions Eqs. (9) and (10)

$$\mathbb{T} = -\frac{\tau_t}{f} + \frac{\tau^r}{f} + 2T_\theta^\theta, \quad (\text{A1})$$

$$\mathbb{T} = \left(\frac{\tau_t}{f}\right)^2 + \left(\frac{\tau^r}{f}\right)^2 - 2\left(\frac{\tau_t}{f}\right)^2 + 2(T_\theta^\theta)^2, \quad (\text{A2})$$

constrains the leading term in  $T_\theta^\theta \equiv T_\phi^\phi$  when  $r \rightarrow r_g$  if the three other components of the EMT scale as  $f^k$ ,  $k < 1$ . Set

$$\Xi_1 := \lim_{r \rightarrow r_g} \tau_t / f^k, \quad \Xi_2 := \lim_{r \rightarrow r_g} \tau^r / f^k, \quad (\text{A3})$$

$$\Xi_3 := \lim_{r \rightarrow r_g} T_\theta^\theta / f^{k-1}, \quad \Xi_4 := \lim_{r \rightarrow r_g} \tau_t^r / f^k, \quad (\text{A4})$$

and focus on the leading terms. The two conditions become

$$-\Xi_1 + \Xi_2 + 2\Xi_3 = 0, \quad \Xi_1^2 + \Xi_2^2 + 2\Xi_3^2 - 2\Xi_4^2 = 0, \quad (\text{A5})$$

Taking  $\Xi_1$  and  $\Xi_2$  as the independent variables we find

$$\Xi_3 = \frac{1}{2}(\Xi_1 - \Xi_2), \quad \Xi_4 = \pm \frac{1}{2} \sqrt{3\Xi_1^2 + 3\Xi_2^2 - 2\Xi_1\Xi_2}. \quad (\text{A6})$$

The Einstein equation (6) does not change; the leading terms of the Misner-Sharp mass are

$$C = r_g - w_1 x^{1/(2-k)}, \quad (\text{A7})$$

where  $w_1 = (-8(2-k)\pi r_g^{3-k}\Xi_1)^{1/(2-k)}$ . The limiting form of Eq. (8) now becomes

$$\partial_r h = 4\pi(\Xi_1 + \Xi_2)r_g^{3-k} \frac{w_1^{k-2}}{x} = -\frac{\Xi_1 + \Xi_2}{2(2-k)\Xi_1 x}, \quad (\text{A8})$$

that results in the leading term

$$h = -\frac{\Xi_1 + \Xi_2}{2(2-k)\Xi_1} \ln \frac{x}{\xi}. \quad (\text{A9})$$

Hence consistency of Eq. (7) imposes

$$-\frac{\Xi_1 + \Xi_2}{2(2-k)\Xi_1} = -\frac{1}{2-k}, \quad (\text{A10})$$

resulting in  $\Xi_1 = \Xi_2$  and

$$\Xi_3 = 0, \quad \Xi_4 = \pm \Xi_1. \quad (\text{A11})$$

#### 2. Regular solutions in $(v, r)$ coordinates.

Existence of the apparent horizon constrains the Misner-Sharp function to have the form

$$C_+ = r_+(v) + w_1^+(v)x^{1-\alpha_1} + w_2^+(v)x^{1-\alpha_1+\alpha_2} + \dots, \quad (\text{A12})$$

where  $x = r - r_+$ , and  $\alpha_1 < 1$ ,  $\alpha_2 > 0$ , while we keep the function  $h$  unconstrained,

$$h_+ = h_+(v) \ln x / \xi(v) + h_1^+(v)x_1^\beta + h_2^+(v)x^{\beta_1+\beta_2} + \dots \quad (\text{A13})$$

Explicit evaluation of the Ricci scalar  $R$  for the metric (12) with the above functions results in a number of the divergent terms, that as  $x \rightarrow 0$  behave as its various powers. The curvature scalar is finite if the coefficients of all such divergent powers cancel. However, it is possible only if  $h_+ = 0$ , as well as all the coefficients of all fractional powers that are less than two.

#### 3. Leading terms of the solutions, $k < 1$

For the EMT components of Eq. (19) with  $k < 1$  (and thus finite  $T_\theta^\theta \equiv T_\phi^\phi$ ) the Einstein equations with divergent terms become

$$\partial_r C \approx -8\pi r_g^2 \Upsilon^2 f^{k-1}, \quad (\text{A14})$$

$$\partial_t C \approx \pm 8\pi r_g^2 e^h \Upsilon^2 f^k, \quad (\text{A15})$$

$$\partial_r h \approx -8\pi r_g \Upsilon^2 f^{k-2}. \quad (\text{A16})$$

The sign choice follows from the observation that the equations have no real solutions if  $\tau_t$  and  $\tau^r$  are  $+\Upsilon^2 f^k$ . The leading terms of the metric functions are then

$$C = r_g(t) - w_1 x^{1/(2-k)}, \quad w_1^{2-k} = 8(2-k)\pi r_g^{3-k} \Upsilon^2, \quad (\text{A17})$$

and

$$h = -\frac{1}{2-k} \ln \frac{x}{\xi}. \quad (\text{A18})$$

Eq. (A15) results in the constraint

$$\pm r'_g = \frac{w_1 \xi^{1/(2-k)}}{r_g}. \quad (\text{A19})$$

It was shown in Section II A that solutions with  $k < 0$  are incompatible with Eq. (15). By following the chain of reasoning that established Eqs. (25) – (27) we show that solutions with  $k > 0$  are also inadmissible. For  $k < 1$  moving from  $(v, r_+(v))$  along the line of constant  $v$  leads to the point  $(t + \delta t, r_g + \delta r)$ , where Eqs. (A17) and (A18) imply

$$\delta t = -\frac{e^{-h}}{f} \Big|_{r=r_g} \delta r = \frac{\delta r}{r'_g}. \quad (\text{A20})$$

For  $k \neq 1$  the analog of Eq. (25) is a contradictory expression

$$\partial_r \theta_v^+ = -\frac{k \Upsilon^2}{f^{1-k}} + \dots \rightarrow -\infty, \quad (\text{A21})$$

showing that solutions with  $0 < k < 1$  are to be excluded.

#### 4. Leading terms of the solutions, $k \geq 1$

For the EMT components of Eq. (19) with  $k \geq 1$  the Einstein equations with divergent terms become

$$\partial_r C \approx 8\pi r_g^2 E(t) f^{k-1}, \quad (\text{A22})$$

$$\partial_t C \approx 8\pi r_g^2 e^h \Phi(t) f^{k\Phi}, \quad (\text{A23})$$

$$\partial_r h \approx 4\pi r_g (E(t) f^{k-2} + P(t) f^{k_P-2}), \quad (\text{A24})$$

for some functions  $E(t)$ ,  $P(t)$  and  $\Phi(t)$  and powers  $k, k_\Phi, k_P \geq 1$ . The leading terms of the Misner-Sharp mass are then

$$C = r_g(t) + 8\pi E r_g^2 x^k. \quad (\text{A25})$$

For  $k > 1$  the constraints of Sec II.B do not apply. In this case

$$f = \frac{x}{r_g} + \dots \quad (\text{A26})$$

Solutions with variable  $r_g(t)$  impose via Eq. (A15) that  $e^h \propto x^{-k_\Phi}$ , i. e. the logarithmic divergence of the function  $h$ . For  $k > 1$  it can be realized only if  $k_P = 1$ . Then

$$h = 4\pi P r_g^2 \ln \frac{x}{\xi}, \quad 4\pi P r_g^2 = -k_\Phi. \quad (\text{A27})$$

Further properties of these solutions are discovered by using the relations between the EMT components (15)–(17). Eq. (15) is satisfied if  $w_+ = 1$ . Eq. (16) then implies  $k_\Phi = 1$  and  $\Phi = -1/(8\pi r_g^2)$ . Eq. (17) is satisfied if  $k \geq 2$ . We see that these solutions are rather peculiar: energy density vanishes at the apparent horizon and the pressure and the flux are determined by the Schwarzschild radius. Moreover, the firewall is present even if  $\Phi < 0$  (Appendix B 3).

For  $k = 1$  and  $k_\Phi > 1$  the equality  $8\pi E r_g^2 = 1$  is still impossible. Assuming that it is true we find that the Misner-Sharp mass in the vicinity of  $r_g$  is

$$C = r_g + x - b^2 x^2 + \dots, \quad f = b^2 x^2 / r_g + \dots, \quad (\text{A28})$$

for some  $b(t)$ . Eq. (7) becomes in the leading order

$$\frac{2b^2 r'_g x}{r_g} = 8\pi \Phi \left( \frac{b^2 x^2}{r_g} \right)^{k_\Phi} e^h, \quad (\text{A29})$$

requiring

$$h = -(2k_\Phi - 1) \ln \frac{x}{\xi} + \dots, \quad (\text{A30})$$

where the higher-order terms are omitted, for time-dependent Schwarzschild radius. Eq. (8) then results in the leading order relation

$$\frac{\partial_x h}{r_g} = \frac{r_g^2}{b^4 x^4} \left( E \frac{b^2 x^2}{r_g} + P \left( \frac{b^2 x^2}{r_g} \right)^{k_P} \right), \quad (\text{A31})$$

resulting in  $1/x$  divergence of the function  $h$ .

Evaluation of the Ricci scalar with these metric functions results in the divergent expression unless  $k_P = k_\Phi = 1$ . It is given in Appendix B 4.

#### Appendix B: Some properties of the solutions

##### 1. Firewall at the apparent horizon, $k < 1$

For a radially infalling massive particle the four-velocity components are related by

$$\dot{T}_A = \frac{\sqrt{F + \dot{R}_A^2}}{e^H F} \approx \frac{|\dot{R}|}{e^H F} + \frac{1}{2|\dot{R}_A| e^H}, \quad (\text{B1})$$

where  $H = h(T_A, R_A)$  and  $F = f(T_A, R_A)$ . For  $k < 1$  this means that the four-velocity of an infalling observer at the leading order is given by

$$u_A^\mu = |\dot{R}_A| \left( \frac{r_g}{w_1 \xi^{1/(2-k)}}, -1, 0, 0 \right), \quad (\text{B2})$$

while the leading terms in the  $(t, r)$  block of the EMT are

$$T_{ab} = -\frac{\Upsilon^2 w_1^{k-2}}{x r_g^{k-2}} \begin{pmatrix} w_1^2 \xi^{2/(2-k)} / r_g^2 & \pm w_1 \xi^{1/(2-k)} / r_g \\ \pm w_1 \xi^{1/(2-k)} / r_g & 1 \end{pmatrix}, \quad (\text{B3})$$

where the upper (lower) sign corresponds to  $r'_g < 0$  ( $r'_g > 0$ ), respectively. The energy density in the frame of the particle is  $\rho_A = T_{\mu\nu} u_A^\mu u_A^\nu$ .

For  $r'_g < 0$  the divergent terms in the energy density cancel out. However, for the expanding apparent horizon the energy density is negative and divergent,

$$\rho_A \approx -\frac{4\dot{R}^2 \Upsilon^2 r_g^{2-k}}{w_1^{2-k} X}, \quad (\text{B4})$$

where  $X = R_A - r_g$ .

##### 2. Firewall at the apparent horizon, $k = 1$ .

The leading terms of the metric functions are

$$C = r_g + 8\pi E r_g^2 x, \quad h = -\ln x / \xi. \quad (\text{B5})$$

The four-velocity of an infalling observer at the leading order is then given by

$$u_A^\mu = |\dot{R}_A| \left( \frac{r_g}{\xi(1 - 8\pi E r_g^2)}, -1, 0, 0 \right), \quad (\text{B6})$$

and the leading terms in the  $(t, r)$  block of the EMT are

$$T_{ab} = \frac{1}{r_g x} \begin{pmatrix} 8\pi E (1 - 8\pi E r_g^2) \xi^2 & r'_g \\ r'_g & -(2 - 8\pi E r_g^2) / (1 - 8\pi E r_g^2) \end{pmatrix}. \quad (\text{B7})$$

In the case of expansion the function  $\xi$  satisfies

$$(1 - 8\pi E r_g^2) \xi = +r'_g r_g, \quad (\text{B8})$$

and the resulting energy density diverges as

$$\rho_A \approx -\frac{4\dot{R}^2}{r_g X}. \quad (\text{B9})$$

For spacetimes of small curvature explicit expressions that bound time-averaged energy density for a geodesic observer were derived in Ref. [27]. For any Hadamard state  $\omega$  and a sampling function  $\mathfrak{f}(\tau)$  of compact support, negativity of the expectation value of the energy density  $\rho_A$  as seen by a geodesic observer on a trajectory  $\gamma(\tau)$  is bounded by

$$\int_{\gamma} \mathfrak{f}^2(\tau) \rho d\tau \geq -B(R, \mathfrak{f}, \gamma), \quad (\text{B10})$$

where  $B > 0$  is a bounded function that depends on the trajectory, the Ricci scalar and the sampling function [27].

Consider a growing apparent horizon,  $r'_g > 0$ . For a macroscopic black hole the curvature at the apparent horizon is low and its radius does not appreciably change while the observer (a massive test particle) moves in its vicinity. Then  $\dot{X} \approx \dot{R}$ , and for a given geodesic trajectory we can choose  $\mathfrak{f} \approx 1$  at the horizon crossing and  $\mathfrak{f} \rightarrow 0$  within the NEC-violating domain. As the trajectory passes through  $X_0 + r_g \rightarrow r_g$  the lhs of Eq. (B10) behaves as

$$\int_{\gamma} \mathfrak{f}^2 \rho_A d\tau \approx - \int_{\gamma} \frac{4\dot{R}^2 d\tau}{r_g X} \approx \int_{\gamma} \frac{4|\dot{R}|dX}{r_g X} \propto \log X_0 \rightarrow -\infty, \quad (\text{B11})$$

where we used  $\dot{R} \sim \text{const.}$  The rhs of Eq. (B10) remains finite, and thus the QEI is violated.

### 3. Firewall at the apparent horizon, $k > 1$ .

Using the results of Appendix A 4 for  $k > 1$ ,  $k_P = k_{\Phi} = 1$  we find that the four-velocity of an infalling observer at the leading order is then given by

$$u_A^{\mu} = |\dot{R}_A| \left( \frac{r_g}{\xi}, -1, 0, 0 \right), \quad (\text{B12})$$

and the leading terms in the  $(t, r)$  block of the EMT are

$$T_{ab} = \begin{pmatrix} E & -(8\pi r_g^2)^{-1} \\ -(8\pi r_g^2)^{-1} & -(4\pi r_g x)^{-1} \end{pmatrix}, \quad (\text{B13})$$

where the minimal allowed power  $k = 2$  was used in  $\tau_t = E f^k$ .

As a results the energy density in the infalling frame

$$\rho_A \approx -\frac{1}{4\pi r_g X}, \quad (\text{B14})$$

diverges even for an evaporating  $k \geq 2$  black hole, and the violation of the QEI is established analogously to Appendix B 1.

### 4. The Ricci scalar, $k = 1$ .

For a dynamical solution in the case  $k = 1$  with the metric functions given by Eqs. (30) and (32) expansion of the Ricci scalar near the apparent horizon gives

$$R = -\frac{(1 - 8\pi E r_g^2)^2 \xi^2 - r_g^2 r_g'^2}{r_g (1 - 8\pi E r_g^2) \xi^2 x} + \mathcal{O}(x^0). \quad (\text{B15})$$

It is finite if and only if Eq. (34) is satisfied.

The Ricci scalar diverges if the evaporating black hole freezes ( $r_g \rightarrow 0$ ), as the regular (as a function of  $x$ ) part of  $R$  contains a clearly divergent term

$$R_0 = \frac{1}{r_g^2 r_g'}. \quad (\text{B16})$$

If the metric function  $h$  has a proportionality coefficient that is different from one (if  $k_{\Phi} > 1$  while  $k_P \geq 1$  and  $k = 1$ ),

$$h = -\lambda \ln \frac{x}{\xi} + \dots, \quad (\text{B17})$$

Eq. (7) implies that  $\lambda = k_{\Phi}$ , and the Ricci scalar contains a potentially divergent term

$$R_{-1} = \frac{\lambda(2\lambda - 1)(1 - 8\pi E r_g^2)}{r_g x}, \quad (\text{B18})$$

that will be zero only if  $\lambda = 0, \frac{1}{2}$  or  $E = (8\pi r_g^2)^{-1}$ .

The two former options (with  $8\pi E r_g^2 < 1$ ) contradict the assumption  $\lambda = k_{\Phi} > 1$ . The third option — the identity  $8\pi E r_g^2 = 1$  — is impossible to satisfy, as demonstrated in Appendix A 4.

- 
- [1] S. W. Hawking and G. F. R. Ellis, *The Large Scale Structure of Space-Time* (Cambridge University Press, 1973).  
[2] V. P. Frolov and I. D. Novikov, *Black Holes: Basic Concepts and New Developments* (Kluwer, Dordrecht, 1998).  
[3] B.-L. Hu and E. Verdaguer, *Semiclassical and Stochastic Gravity: Quantum Field Effects on Curved Spacetime* (Cambridge University Press, 2020).  
[4] N. D. Birrel and P. C. W. Davies, *Quantum Fields in Curved Space* (Cambridge University Press, Cambridge, 1986).  
[5] J. F. Donoghue, arXiv:1209.3511 (2012); N. E. J. Bjerrum-

- Bohr, J. F. Donoghue, B. R. Holstein, L. Planté, and P. Vanhove, Phys. Rev. Lett. **114**, 061301 (2015).  
[6] C. Rovelli and F. Vidotto, *Covariant Loop Quantum Gravity* (Cambridge University Press, Cambridge, 2014).  
[7] P. Martín-Moruno and M. Visser, *Classical and Semi-classical Energy Conditions*, in *Wormholes, Warp Drives and Energy Conditions*, edited by F. N. S. Lobo (Springer, New York, 2017), p. 193.  
[8] E.-A. Kontou and K. Sanders, arXiv:2003.01815 (2020).  
[9] V. Cardoso and P. Pani, Nature Astr. **1**, 586 (2017); V. Cardoso



- and P. Pani, *Living Rev. Relat.* **22**, 4 (2019).
- [10] L. Barack, V. Cardoso, S. Nissanke, and T. P. Sotiriou (eds.), *Black holes, gravitational waves and fundamental physics: a roadmap*, *Class. Quant. Grav.* **36**, 143001 (2019).
- [11] P. Chen, Y. C. Ong, and D.-h. Yeom, *Phys. Reports* **603**, 1 (2015).
- [12] C. Bambi, *Black Holes: a Laboratory for Testing Strong Gravity* (Springer, Singapore, 2017); C. Bambi, *Ann. Phys. (Berlin)* **530**, 1700430 (2018).
- [13] LIGO Scientific Collaboration and Virgo Collaboration, *Phys. Rev. X* **9**, 031040 (2019).
- [14] Event Horizon Telescope Collaboration, *Astrophys. J. Lett.* **875**, L1 (2019).
- [15] R. B. Mann, *Black Holes: Thermodynamics, Information, and Firewalls* (Springer, New York, 2015); V. Baccetti, V. Hussain and D. R. Terno, *Entropy* **19**, 17 (2017).
- [16] D. Harlow, *Rev. Mod. Phys.* **88**, 015002 (2016); W. G. Unruh and R. M. Wald, *Rep. Prog. Phys.* **80** 092002 (2017); D. Marolf *Rep. Prog. Phys.* **80**, 092001 (2017).
- [17] E. Curiel, *Nature Astron.* **3**, 27 (2019).
- [18] V. Faraoni, *Cosmological and Black Hole Apparent Horizons*, (Springer, Heidelberg, 2015).
- [19] V. P. Frolov, arXiv:1411.6981 (2014).
- [20] V. Baccetti, R. B. Mann, S. Murk, and D. R. Terno, *Phys. Rev. D* **99**, 124014 (2019).
- [21] V. Faraoni, G. F. R. Ellis, J. T. Firouzjaee, A. Helou, and I. Musco, *Phys. Rev. D* **95**, 024008 (2017).
- [22] V. Baccetti, S. Murk, and D. R. Terno, *Phys. Rev. D* **100**, 064054 (2019).
- [23] D. R. Terno, *Phys. Rev. D* **100**, 124025 (2019).
- [24] C. W. Misner and D. H. Sharp, *Phys. Rev.* **136** B571 (1964).
- [25] P. T. Chruściel, J. L. Costa, and M. Heusler, *Living Rev. Rel.* **15**, 7 (2012).
- [26] C. J. Fewster, *Quantum Energy Inequalities*, in *Wormholes, Warp Drives and Energy Conditions*, edited by F. N. S. Lobo (Springer, New York, 2017), p. 215.
- [27] E.-A. Kontou and K. D. Olum, *Phys. Rev. D* **91**, 104005 (2015).
- [28] J. M. Bardeen, *Phys. Rev. Lett.* **46**, 382 (1981).
- [29] R. Brout, S. Massar, R. Parentani, and P. Spindel, *Phys. Rep.* **260**, 329 (1995).
- [30] A. Levi and A. Ori, *Phys. Rev. Lett.* **117**, 231101 (2016).
- [31] H. Kawai, Y. Matsuo, Y. Yokokura, *Int. J. Mod. Phys. A* **28**, 1350050 (2013).
- [32] I. Nagle, R. B. Mann and D. R. Terno, *Nucl. Phys. B* **936**, 18 (2018).
- [33] P. Chen, W. G. Unruh, C.-H. Wu, and D.-h. Yeom, *Phys. Rev. D* **97**, 064045 (2018).
- [34] R. A. Rosen, *JHEP* **10(2017)**, 206 (2017).
- [35] J. M. Bardeen, in *Proceedings of International Conference GR5*, (Tbilisi, USSR, 1968), p. 174 (cited in [11]).
- [36] V. P. Frolov and G. A. Vilkovisky, *Phys. Lett.* **106B**, 307 (1981).
- [37] S. A. Hayward, *Phys. Rev. Lett.* **96**, 031103 (2006).
- [38] V. P. Frolov, *JHEP* **05(2014)**, 049 (2014).
- [39] R. Carballo-Rubio, F. Di Filippo, S. Liberati, C. Pacillo, and M. Visser, *JHEP* **07(2018)** 023 (2018).
- [40] R. Brustein and A. J. M. Medved, *Phys. Rev. D* **99**, 064019 (2019).
- [41] S. D. Mathur, *Fortsch. Phys.* **53**, 793 (2005).
- [42] S. Ansoldi, arXiv:0802.0330 [gr-qc] (2008).
- [43] R. Carballo-Rubio, F. Di Filippo, S. Liberati, and M. Visser, arXiv:1908.03261 (2019); R. Carballo-Rubio, F. Di Filippo, S. Liberati, and M. Visser, arXiv:1911.11200 (2019).
- [44] V. P. Frolov, M. Markov, and V. F. Mukhanov, *Phys. Lett. B* **216**, 272 (1989).
- [45] T. De Lorenzo, C. Pacilio, C. Rovelli, and S. Speziale, *Gen. Relat. Grav.* **47**, 41 (2015).
- [46] R. Brustein and A. J. M. Medved, *Fortsch. Phys.* **67**, 1900058 (2019).